JOURNAL OF SPACECRAFT AND ROCKETS
Vol. 32, No. 1, January–February 1995

Vehicle-and-Trajectory Optimization of Nuclear Electric Spacecraft for Lunar Missions

Craig A. Kluever*
University of Missouri—Columbia/Kansas City, Kansas City, Missouri 64110-2499
and
Bion L. Pierson†
Iowa State University, Ames, Iowa 50011-3231

A new combined vehicle-and-trajectory optimization problem is solved for a low-thrust nuclear-electric-propulsion spacecraft whose motion is governed by restricted three-body-problem dynamics for the Earth-moon system. The problem involves computing the optimal spacecraft sizing parameters and trajectory design variables that result in the maximum payload for a fixed-trip-time, planar transfer from circular low Earth orbit to circular low-lunar orbit. In particular, the optimal specific impulse and input power are computed. The detailed vehicle-and-trajectory optimization approach is effective in solving a complex interactive problem that is important to both spacecraft and mission designers. Several numerical solutions are obtained for a wide range of trip times.

Nomenclature

a_T = thrust acceleration, m/s^2
b = propellant-dependent coefficient, nondimensional
c = engine exhaust velocity, km/s
D = distance of Earth-moon separation, km
d = propellant-dependent coefficient, km/s
f = state differential-equation vector
g = sea-level gravitational acceleration, m/s^2
H = Hamiltonian
I_{sp} = specific impulse, s
J = performance index, kg
K_t = tankage fraction, nondimensional
m = spacecraft mass, kg
m_{net} = net mass of spacecraft, kg
m_{pp} = mass of power and propulsion system, kg
m_{prop} = propellant mass, kg
m_{tank} = mass of tank and propellant feed system, kg
P = input power, kW
r = radial position, km
t = time, days
T = thrust magnitude, N
t_{escape} = total duration of the powered Earth-escape spiral, $\Delta t_{QC_1} + \Delta t_e$, days
$t_{capture}$ = total duration of the powered moon-capture spiral, $\Delta t_c + \Delta t_{QC_3}$, days
u = thrust steering angle measured from the local horizon to the thrust vector, deg
v_r = radial velocity, km/s
v_θ = circumferential velocity, km/s
x = state vector
Δt_{coast} = duration of the translunar coast trajectory, days
Δt_c = duration of the powered, numerically simulated moon-capture trajectory, days
Δt_e = duration of the powered, numerically simulated Earth-escape trajectory, days
Δt_{QC} = duration of the powered quasicircular transfer, days
ΔV = velocity difference between two concentric circular orbits, km/s
α = specific mass of the power and propulsion system, kg/kW
η = thruster efficiency, nondimensional
θ = polar angle, deg
λ = costate vector
μ = gravitational parameter, km^3/s^2
τ = time for start of Moon-capture spiral, $t_F - t_{capture}$, days
ω = angular rate of Earth-moon system, rad/s

Subscripts

0 = initial (low Earth orbit)
1 = with respect to the Earth (powered trajectory)
2 = with respect to the Earth (coast trajectory)
3 = with respect to the moon (powered trajectory)
f = end of quasicircular transfer
F = final (low-lunar orbit)
GEO = geosynchronous circular orbit
HLO = high lunar circular orbit
i = start of quasicircular transfer
LEO = low Earth circular orbit
LLO = low lunar circular orbit

Received Sept. 7, 1993; revision received May 26, 1994; accepted for publication May 26, 1994; presented as Paper 94-3255 at the 30th AIAA/ASME/SAE/ASEE Joint Propulsion Conference, Indianapolis, IN, June 27–29, 1994.

*Assistant Professor, Department of Mechanical and Aerospace Engineering. Member AIAA.
†Professor, Department of Aerospace Engineering and Engineering Mechanics. Associate Fellow AIAA.

Introduction

LOW-THRUST electric propulsion systems have been identified as an efficient means for performing space missions. Spacecraft propelled by low-thrust engines are capable of delivering a greater payload fraction than spacecraft using conventional chemical propulsion systems. Recent low-thrust research has focused on a particular electric propulsion candidate, namely nuclear electric propulsion (NEP) for a range of piloted and cargo lunar and Mars missions.[1,2] Jaffe[3] has investigated the use of an NEP vehicle for near-Earth orbital transfer. An important aspect of vehicle and mission design is the optimization of both the propulsion-system parameters and the spacecraft trajectory. Unlike pure trajectory optimization problems, this problem exhibits a coupled interaction between propulsion-system optimization and trajectory optimization. Trajectory optimization for low-thrust missions has typically involved computing minimum-fuel trajectories for vehicles with constant propulsion-system parameters. Golan and Breakwell[4] and Enright and Conway[5] have investigated minimum-fuel Earth-moon trajectories for a fixed low-thrust spacecraft. Gilland[6] has investigated combined propulsion-system and trajectory optimization problems for lunar and Mars missions, using approximations in order to simplify

the detailed interaction between optimal trajectory and optimal vehicle parameter. In particular, the optimal propulsion-system parameters were computed for a lunar cargo NEP vehicle by utilizing a simple analytical expression for the required velocity increment for the lunar transfer trajectory.[7] Burton and Wassgren[8] have investigated the optimal mass distribution of a low-thrust electric-propulsion spacecraft for a near-Earth orbital transfer. The transfer is approximated by utilizing a characteristic velocity increment, and this approach is similar to the method of Ref. 6.

This paper presents several solutions to a detailed coupled vehicle-trajectory optimization problem for a low-thrust planar transfer from a circular low Earth parking orbit (LEO) to a circular low lunar parking orbit (LLO). The combined vehicle-and-trajectory optimization problem involves maximizing the spacecraft's payload for a given initial mass in LEO and fixed transfer time. The vehicle sizing feature requires computing the optimal specific impulse and the optimal electric power input to the thrusters. These two engine parameters determine the thrust magnitude, propellant mass flow rate, and thruster efficiency for the NEP vehicle. The LEO-LLO transfer is assumed to consist of a continuous-thrust spiral Earth-escape trajectory, followed by a translunar coast arc, and finally a continuous-thrust spiral moon-capture trajectory. The trajectory optimization involves finding the thrust steering-angle histories during the Earth-escape and moon-capture spirals.

Payload and Propulsion-System Calculations

The objective of the combined vehicle-and-trajectory optimization problem is to maximize the net mass of the spacecraft for a fixed-time transfer from LEO to LLO. The net mass m_{net} is defined as

$$m_{\text{net}} = m_0 - m_{\text{prop}} - m_{\text{tank}} - m_{\text{pp}} \tag{1}$$

The spacecraft's net mass represents the usable mass for payload plus the basic spacecraft structural mass. The basic structural mass can be computed as a percentage (5–10%) of the initial mass m_0 and is therefore considered independent of the tank mass, engine mass, and power-system mass.[1] The tank mass m_{tank} and the mass of the power and propulsion system, m_{pp}, are proportional to the total propellant mass m_{prop} and electric power input P, respectively[6]:

$$m_{\text{tank}} = K_t m_{\text{prop}} \tag{2}$$

$$m_{\text{pp}} = \alpha P \tag{3}$$

The vehicle sizing parameters K_t and α as well as m_0 are considered constant for the NEP lunar cargo vehicle, according to Refs. 2 and 9. It is assumed that xenon is utilized as the propellant for the NEP vehicle. The vehicle parameters are derived by scaling the current technology level for space nuclear power and ion thrusters.[2,9] A scaled-up or "growth" reactor system is presented in Ref. 9 for the multimegawatt power range. The power and propulsion system parameters represent a projected technology level for an NEP lunar cargo spacecraft in the 2010 time frame. The constant numerical values for these vehicle parameters are

$$K_t = 0.05 \qquad \text{(nondimensional)}$$

$$\alpha = 7.3 \text{ kg/kW}$$

$$m_0 = 123{,}000 \text{ kg}$$

Using these vehicle sizing parameters, we can rewrite the net mass as

$$m_{\text{net}} = m_0 - (1 + K_t)m_{\text{prop}} - \alpha P \tag{4}$$

The total propellant mass m_{prop} is the product of the constant mass flow rate $\dot{m}$ and the total engine-on time:

$$m_{\text{prop}} = \dot{m}(t_{\text{escape}} + t_{\text{capture}}) \tag{5}$$

The remainder of the propulsion-system parameters are completely determined by I_{sp} and P. These design parameters are regarded as fixed over the duration of the mission. Equivalently, this assumes a single operating point and no engine throttling. Although constant $\dot{m}$ is not optimal, it does represent a realistic NEP vehicle. The thrust magnitude T is[10]

$$T = (2\eta P/c) \tag{6}$$

The exhaust velocity is

$$c = I_{\text{sp}} g \tag{7}$$

The thruster efficiency for ion thrusters is determined by the relation[6]

$$\eta = (bc^2/c^2 + d^2) \tag{8}$$

where b and d are determined from theoretical models and experimental data.[6] For xenon, the nondimensional coefficient b equals 0.81 and the coefficient d equals 13.5 km/s.

The propellant mass flow rate is determined from the thrust magnitude and exhaust velocity:

$$\dot{m} = (T/c) \tag{9}$$

The mass flow rate $\dot{m}$ is considered positive and represents mass flow out of the vehicle.

The net mass and all spacecraft propulsion-system parameters can now be expressed solely in terms of the independent variables I_{sp}, P, and thrust arc durations t_{escape} and t_{capture}. These variables constitute some of the design variables for the vehicle-and-trajectory optimization problem. After substituting Eqs. (7) and (8) into Eqs. (6) and (9), we obtain for the thrust magnitude and propellant mass flow rate

$$T = 2bg\frac{I_{\text{sp}}P}{I_{\text{sp}}^2 g^2 + d^2} \tag{10}$$

$$\dot{m} = 2b\frac{P}{I_{\text{sp}}^2 g^2 + d^2} \tag{11}$$

Finally, after substituting Eqs. (11) and (5) into Eq. (4), we obtain for the net mass

$$m_{\text{net}} = m_0 - \left[(1 + K_t)\frac{2bP}{I_{\text{sp}}^2 g^2 + d^2}(t_{\text{escape}} + t_{\text{capture}}) + \alpha P\right] \tag{12}$$

Maximum-Payload Problem

As previously described, the objective of the combined vehicle-and-trajectory optimization problem is to maximize the payload or net mass of the spacecraft for a one-way, fixed-trip-time LEO-LLO transfer. Since most optimization software is designed to minimize an objective function, this maximization problem is treated by minimizing the negative of the net mass. Since m_0 is a constant, it can be removed from the performance index. A complete problem statement for the combined vehicle-and-trajectory problem is as follows: Find the vehicle parameters P and I_{sp}, the thrust steering angles $u_1(t)$ and $u_3(t)$, and the thrust durations t_{escape} and t_{capture} that minimize

$$J = (1 + K_t)\frac{2bP}{I_{\text{sp}}^2 g^2 + d^2}(t_{\text{escape}} + t_{\text{capture}}) + \alpha P \tag{13}$$

where K_t, b, d, g, and α are all given constants, subject to

$$\dot{r}_1 = v_{r_1} \tag{14}$$

$$\dot{v}_{r_1} = \frac{v_{\theta_1}^2}{r_1} - \frac{\mu_1}{r_1^2} - \frac{\mu_2(r_1 + D\cos\theta_1)}{r_{\text{moon-S/C}}^3} + \frac{\mu_2 \cos\theta_1}{D^2} + a_{T_1}\sin u_1 + 2\omega v_{\theta_1} + \omega^2 r_1 \tag{15}$$

$$\dot{v}_{\theta_1} = \frac{\mu_2 D\sin\theta_1}{r_{\text{moon-S/C}}^3} - \frac{\mu_2 \sin\theta_1}{D^2} + a_{T_1}\cos u_1 - 2\omega v_{r_1} - \frac{v_{r_1} v_{\theta_1}}{r_1} \tag{16}$$

$$\dot{\theta}_1 = \frac{v_{\theta_1}}{r_1} \tag{17}$$

where $r_{\text{moon-S/C}} = \left(r_1^2 + 2Dr_1\cos\theta_1 + D^2\right)^{1/2}$ and

$$a_{T_1} = \frac{T}{m_0 - \dot{m}t}, \qquad 0 \le t \le t_{\text{escape}}$$

and subject to

$$\dot{r}_2 = v_{r_2} \tag{18}$$

$$\dot{v}_{r_2} = \frac{v_{\theta_2}^2}{r_2} - \frac{\mu_1}{r_2^2} - \frac{\mu_2(r_2 + D\cos\theta_2)}{r_{\text{moon-S/C}}^3} + \frac{\mu_2\cos\theta_2}{D^2} + 2\omega v_{\theta_2} + \omega^2 r_2 \tag{19}$$

$$\dot{v}_{\theta_2} = \frac{\mu_2 D\sin\theta_2}{r_{\text{moon-S/C}}^3} - \frac{\mu_2\sin\theta_2}{D^2} - 2\omega v_{r_2} - \frac{v_{r_2}v_{\theta_2}}{r_2} \tag{20}$$

$$\dot{\theta}_2 = \frac{v_{\theta_2}}{r_2} \tag{21}$$

$$\dot{r}_3 = v_{r_3} \tag{22}$$

$$\dot{v}_{r_3} = \frac{v_{\theta_3}^2}{r_3} - \frac{\mu_2}{r_3^2} - \frac{\mu_1(r_3 - D\cos\theta_3)}{r_{\text{Earth-S/C}}^3} - \frac{\mu_1\cos\theta_3}{D^2} + a_{T_3}\sin u_3 + 2\omega v_{\theta_3} + \omega^2 r_3 \tag{23}$$

$$\dot{v}_{\theta_3} = \frac{-\mu_1 D\sin\theta_3}{r_{\text{Earth-S/C}}^3} + \frac{\mu_1\sin\theta_3}{D^2} + a_{T_3}\cos u_3 - 2\omega v_{r_3} - \frac{v_{r_3}v_{\theta_3}}{r_3} \tag{24}$$

$$\dot{\theta}_3 = \frac{v_{\theta_3}}{r_3}, \tag{25}$$

where $r_{\text{Earth-S/C}} = \left(r_3^2 - 2Dr_3\cos\theta_3 + D^2\right)^{1/2}$ and

$$a_{T_3} = \frac{T}{m(t_{\text{escape}}) - \dot{m}(t - \tau)}, \qquad \tau \le t \le t_F$$

and subject to the inequality constraint

$$3000 \le I_{sp} \le 7000 \text{ s} \tag{26}$$

with the boundary conditions at $t = 0$

$$r_1(0) = r_{1_0} \tag{27}$$

$$v_{r_1}(0) = 0 \tag{28}$$

$$v_{\theta_1}(0) = \sqrt{\frac{\mu_1}{r_{1_0}}} - \omega r_{1_0} \tag{29}$$

and the boundary conditions at $t = t_{\text{escape}}$

$$r_2(t_{\text{escape}}) = r_1(t_{\text{escape}}) \tag{30}$$

$$v_{r_2}(t_{\text{escape}}) = v_{r_1}(t_{\text{escape}}) \tag{31}$$

$$v_{\theta_2}(t_{\text{escape}}) = v_{\theta_1}(t_{\text{escape}}) \tag{32}$$

$$\theta_2(t_{\text{escape}}) = \theta_1(t_{\text{escape}}) \tag{33}$$

and the boundary conditions at $t = \tau$

$$r_3(\tau) = r_2(\tau) \tag{34}$$

$$v_{r_3}(\tau) = v_{r_2}(\tau) \tag{35}$$

$$v_{\theta_3}(\tau) = v_{\theta_2}(\tau) \tag{36}$$

$$\theta_3(\tau) = \theta_2(\tau) \tag{37}$$

and the boundary conditions at $t = t_F$

$$r_3(t_F) = r_{3_F} \tag{38}$$

$$v_{r_3}(t_F) = 0 \tag{39}$$

$$v_{\theta_3}(t_F) = \sqrt{\frac{\mu_2}{r_{3_F}}} - \omega r_{3_F} \tag{40}$$

The first set of four differential equations, Eqs. (14–17), are the equations of motion for the thrusting spacecraft in an Earth-centered, rotating polar coordinate system for the restricted three-body-problem dynamics.[11] The classical restricted three-body problem is defined by two point masses, in this case the Earth and the moon, revolving with a constant angular rate in circular orbits about their common center of mass. The third body, in this case the spacecraft, is considered to be of negligible mass in comparison with the primary bodies and therefore does not influence their motion. The three-body problem accurately describes the Earth-moon system, since the moon's orbit about the common center of mass is nearly circular, with an eccentricity of 0.05. The values for the thrust T and mass flow rate $\dot{m}$ in the expression for the thrust acceleration a_T were previously defined by Eqs. (10) and (11). The second set of four differential equations, Eqs. (18–21), are the three-body equations of motion for the coasting spacecraft in the Earth-centered frame. The third set of four differential equations, Eqs. (22–25), are the equations of motion for the thrusting spacecraft in a moon-centered, rotating polar coordinate system.

The initial and final conditions are for low circular parking orbits about the Earth and moon as shown by Eqs. (27–29) and Eqs. (38–40), respectively. The boundary conditions (30–33) and (34–37) indicate the required matching conditions between the powered and unpowered trajectory segments. The specific impulse for xenon is bounded [Eq. (26)] by the range of input voltages for the low-thrust engine.[6]

Thrust Steering-Angle Parametrization

In general, an optimal-control problem may be solved using either direct or indirect methods. An indirect method involves applying the calculus of variations and solving the corresponding two-point boundary-value problem (2PBVP). This is usually an extremely difficult problem except in the case of a simple dynamic system. A direct method utilizes a parametrization of the control and attempts to reduce the performance index directly at each iteration. Since our maximum-net-mass problem involves sensitive system dynamics and a dual coordinate frame, a direct optimization method is used here. The optimal-control problem is replaced with an approximate nonlinear programming problem with the continuous control history replaced with a finite number of parameters. A typical approach to parametrizing the control is to utilize linear or cubic spline interpolation through a fixed number of control points. For the very long-duration spiral trajectories, this technique would require a very large number of control points. A more efficient and accurate technique is to utilize the necessary conditions from optimal-control theory[12] to parametrize the control histories. As a result, the optimal thrust steering angle u^* is parametrized by the costate differential equations. To illustrate this procedure, we derive here the steering parametrization for the Earth-escape spiral phase using the dynamics defined in the Earth-centered rotating frame. For simplicity, the subscript 1 is dropped from the variables.

The Hamiltonian is

$$H(x, u, \lambda, t) = \lambda^T f(x, u, t) \tag{41}$$

The costate differential equations are[12]

$$\dot{\lambda} = -\left(\frac{\partial H}{\partial x}\right)^T \tag{42}$$

The optimal thrust steering angle u^* is determined by the stationarity condition[12]

$$\frac{\partial H}{\partial u} = 0 \tag{43}$$

Utilizing Eqs. (15) and (16), we obtain from the stationarity condition

$$\lambda_{v_r} a_T \cos u - \lambda_{v_\theta} a_T \sin u = 0 \quad \Rightarrow \quad u^* = \tan^{-1}\left(\frac{-\lambda_{v_r}}{-\lambda_{v_\theta}}\right) \tag{44}$$

where λ_{v_r} and λ_{v_θ} correspond to the radial and circumferential velocity costates, respectively. The negative signs in Eq. (44) are chosen to satisfy the Legendre-Clebsch condition. The thrust steering angle u is parametrized by selecting initial costate values and integrating the costate differential equations forward in time along with the state equations.[13] The initial value of the polar-angle costate, λ_θ, is zero, since the initial polar angle is free. Therefore, the three initial costate elements (λ_r, λ_{v_r}, and λ_{v_θ}) are the parameters in the direct method. A similar costate parametrization is used for the steering angle for the lunar capture spiral as well.

Edelbaum Approximation for Quasicircular Transfers

Preliminary attempts to solve the vehicle-and-trajectory optimization problem resulted in convergence problems due to the very long-duration, very nearly circular spirals about both the Earth and the moon. The long spiral times are caused by the range of very low T/W ratios available for the NEP spacecraft. Another problem is the sensitive parametrization of the thrust steering angle. Since the steering-angle history is determined by the very sensitive and oscillatory costate-system, even small perturbations to the initial costates in LEO produce very different control-angle histories and therefore different trajectories. In addition, the hundreds of tight low-altitude spirals require thousands of integration steps and therefore greatly increase the computational cost of solving the problem.

In order to improve the convergence properties and reduce the computational load, the maximum-payload problem for the NEP vehicle is solved from a geosynchronous-altitude, circular Earth orbit (GEO) to a high-altitude, circular lunar orbit (HLO). Choosing these boundary conditions eliminates hundreds of nearly circular orbits about the Earth and Moon from the complete simulation. The slowly opening, near-circular spiral trajectories from 407-km-altitude LEO to GEO and from 100-km-altitude LLO to 2038-km-altitude HLO are approximated by analytical equations developed by Edelbaum[14] for minimum-propellant, low-thrust transfer problems between inclined circular orbits. Edelbaum obtained a closed-form solution by making two additional assumptions: 1) the orbits remain quasicircular during the transfer from a lower circular orbit to a higher circular orbit, and 2) the thrust steering angle is constant during each revolution. Edelbaum has shown that there is very little difference between the analytical solutions and the true, numerically calculated optimal transfer.[14]

In order to demonstrate the validity of these approximations, we numerically simulated two trajectories, an Earth-escape spiral and a moon-capture spiral. The two trajectories are computed for a fixed NEP spacecraft with a power input of 5000 kW and an I_{sp} of 5000 s. The thrust is directed along the velocity vector throughout the trajectory. The escape trajectory with tangent steering required 40.7 days and 261 revolutions to spiral from LEO to GEO altitude. The final orbit was very nearly circular and yielded a final radial velocity component of 0.04 km/s and a final eccentricity of 0.01. The purpose of the second trajectory is to allow a reasonable selection of the high-lunar-orbit altitude. The capture trajectory was integrated backwards in time from LLO, and we observed that the radial velocity component remained very small until the spiral time reached about 4 days. After 4 days and 28 revolutions about the moon in backward-in-time spiraling from LLO, the radial velocity was −0.02 km/s and the altitude above the moon was 2038 km.

Edelbaum's analytical expression is used to calculate the minimum time required to transfer from LEO to GEO and from HLO to LLO. Edelbaum's analytical expression for a planar circle-to-circle transfer is the simple rocket equation:[14]

$$(m_f/m_i) = e^{-\Delta V/g I_{sp}} \tag{45}$$

where ΔV is a constant for the two quasicircular planar transfers. In particular, $\Delta V_1 = V_{LEO} - V_{GEO}$ for the LEO-quasicircular transfer, and $\Delta V_3 = V_{LLO} - V_{HLO}$ for the LLO quasicircular transfer. Therefore, by varying I_{sp}, the final-to-initial mass ratio m_f/m_i is altered for the quasicircular transfer between fixed circular orbits. The trip time for the quasicircular transfer is computed from the mass ratio and the constant propellant mass flow rate. Since the mass flow rate $\dot{m}$ is determined by P and I_{sp} as given by Eq. (11), the trip time for the quasicircular transfer becomes

$$\Delta t_{QC} = \frac{m_i\left(I_{sp}^2 g^2 + d^2\right)}{2bP}\left[1 - e^{-\Delta V/g I_{sp}}\right] \tag{46}$$

Edelbaum's analytical expression for the long-duration quasicircular transfers therefore contributes to the computation of m_{prop} through Eq. (5) with the thrust arc durations t_{escape} and $t_{capture}$ defined as

$$t_{escape} = \Delta t_{QC_1} + \Delta t_e \tag{47}$$

$$t_{capture} = \Delta t_c + \Delta t_{QC_3} \tag{48}$$

The quasicircular transfer times Δt_{QC_1} and Δt_{QC_3} also contribute to the computation of the total trip time:

$$t_F = \Delta t_{QC_1} + \Delta t_e + \Delta t_{coast} + \Delta t_c + \Delta t_{QC_3} \tag{49}$$

Utilization of the Minimum-Propellant Solution

A low-thrust transfer from LEO to LLO is a long-duration trajectory with slowly developing spirals about each primary body. The sensitive restricted three-body dynamics, coupled with the strict terminal-state constraints requiring a circular lunar orbit, makes the complete LEO-LLO trajectory very sensitive to initial guesses for the spacecraft control. The prospect of obtaining the optimal vehicle-and-trajectory combination by solving a single optimization problem numerically seems very remote. Therefore, the combined vehicle-and-trajectory optimization problem is solved by utilizing a minimum-propellant solution as the initial guess for the trajectory design variables. The minimum-propellant solution is described in detail in Ref. 15 and was obtained for a fixed-parameter NEP spacecraft defined by Refs. 2 and 9 with a 5000-kW power system. The fixed NEP vehicle also utilized xenon as the propellant with an I_{sp} of 5000 s. The minimum-propellant solution for the fixed NEP spacecraft was obtained by utilizing a three-stage approach, which involves solving a hierarchy of subproblems.[13] The first subproblem involves computing several maximum-energy, continuous-thrust Earth-escape and moon-capture trajectories. The second subproblem is to compute a suboptimal, all-coasting, translunar trajectory between curve-fitted boundary conditions provided by the first subproblem. Finally, the complete minimum-propellant trajectory is obtained using a "hybrid" direct-indirect method,[13] which utilizes the costate time histories to parametrize the thrust steering history.

The requirement for the trajectory to terminate in a low lunar circular orbit greatly increases the sensitivity of the problem to the initial guesses for a one-way GEO-HLO numerical integration. Therefore, the GEO-HLO trajectory is divided into two trajectory segments. The first segment starts in GEO and consists of the Earth-escape spiral and the translunar coast arc, and the second trajectory segment starts in HLO and consists of the moon-capture spiral. The numerical sensitivity of the problem is reduced by matching the two trajectory segments near the lunar sphere of influence (SOI), where the gravity fields of the Earth and moon are nearly equal. The Earth-escape state and costate differential equations are numerically integrated forward in time in the Earth-centered rotating frame. The moon-capture state and costate differential equations are numerically integrated backwards in time from HLO in the moon-centered rotating frame. Although it is not standard practice, this matching technique is essential for the satisfaction of the sensitive boundary conditions. The forward and backward numerical integration with intermediate matching is detailed in Ref. 13.

The nonlinear programming problems are solved numerically using sequential quadratic programming (SQP), which is a constrained parameter optimization method.[16] The SQP algorithm used is DNCONF from the International Mathematics and Statistics

Library[17] (IMSL) and is based on Schittkowski's nonlinear code NLPQL.

The hybrid direct-indirect method for the free-end-time, minimum-propellant solution of the fixed NEP vehicle is modified to solve the fixed-end-time, maximum-net-mass problem. The vehicle parameters P and I_{sp} are additional SQP design variables in the direct-indirect method. The SQP performance index is the sum of the total propellant mass, tank mass, and power and propulsion system mass as previously indicated by Eq. (13), and its minimum results in the maximum net mass. The other SQP design variables include the initial control values $u(0)$ and $\dot{u}(0)$ in GEO and HLO, the initial and final polar angles in GEO and HLO, and the durations of the numerically simulated Earth-escape spiral (Δt_e), the coast arc (Δt_{coast}), and the numerically simulated moon-capture spiral (Δt_c). The initial costates are derived from the initial control values $u(0)$ and $\dot{u}(0)$ using a costate-control transformation.[18] Four SQP equality constraints are imposed to force position- and velocity-vector matching between the two trajectory segments near the lunar SOI. A fifth SQP equality constraint requires the computed total trip time to correspond to the desired fixed end time. Thus, our approximate nonlinear programming problem involves eleven design variables and five equality constraints.

Results

The first maximum-net-mass solution is found for a fixed trip time of 72.5 days, which closely corresponds to the optimal trip time for the free-end-time, minimum-propellant solution for the fixed NEP vehicle. Since the spacecraft system parameters I_{sp} and P are fixed, the minimum-propellant problem allows for a free end time, and the result is a total trip time of 72.44 days. Both the maximum-net-mass and the minimum-propellant NEP vehicle problem start with an initial spacecraft mass in LEO of 123,000 kg. The minimum-propellant solution is used as the initial guess for the maximum-payload problem with variable I_{sp} and P.

The modified direct-indirect method converges to a maximum-net-mass solution after over 100 SQP iterations. The I_{sp} and power are substantially changed from the initial guesses of 5000 s and 5000 kW to the optimal values of 3641.4 s and 3614.7 kW, respectively. The optimal net mass for the 72.5-day transfer is 71,370.4 kg. The net mass for the minimum-propellant solution from Ref. 15 is 67,836.4 kg. The maximum-net-mass solution therefore displays a 5.21% increase in payload over the minimum-propellant solution. The payload fraction, the ratio of the net mass to the initial spacecraft mass in LEO is 0.580 for the maximum-net-mass solution. Therefore, 41.98% of the initial spacecraft mass in LEO is propellant, tank mass, and power and propulsion system mass. In comparison, the payload fraction for the minimum-propellant solution is 0.552. The maximum-net-mass solution requires 24,040.0 kg of propellant to complete the transfer, which is 35.2% more propellant than the 17,774.9-kg propellant mass for the minimum-propellant solution. The ratio of final mass to initial mass is 0.805 for the maximum-net-mass solution, as compared to 0.855 for the minimum-propellant solution. Although the minimum-propellant trajectory exhibits a higher mass ratio, the power and propulsion system is more massive for the minimum-propellant solution and therefore detracts from the vehicle's payload capability.

The optimal trajectory for the maximum-net-mass problem is slightly different from the minimum-propellant trajectory for a fixed NEP vehicle. The optimal NEP vehicle completes 261 revolutions about the Earth in 42.75 days during the Edelbaum approximation for the LEO-GEO quasicircular transfer, compared to a 40.64-day LEO-GEO transfer for the minimum-propellant trajectory. The numerically simulated trajectory for the maximum-net-mass transfer completes 6.0 revolutions about the Earth during the escape spiral from circular GEO to the start of the translunar coast arc. The maximum-net-mass NEP vehicle completes 9.5 revolutions about the moon during the 7.11-day capture spiral that terminates at HLO. In comparison, the minimum-propellant NEP vehicle's translunar coast arc is over twice as long, and the moon-capture spiral to HLO lasts 6.56 days. The quasicircular transfer from HLO to LLO approximated by Edelbaum's analytical equation is nearly the same for both NEP vehicle trajectories. The trip time for the numerically simulated GEO-HLO transfer is 25.78 days for the maximum-payload trajectory and 27.87 days for the minimum-propellant trajectory. A comparison between the maximum-net-mass solution and the fixed-vehicle, minimum-propellant solution is presented in Table 1. The maximum-net-mass GEO-HLO trajectory is shown in the Earth-centered, rotating frame in Fig. 1.

Several maximum-net-mass trajectories are found for a range of trip times by utilizing the current solution as the initial guess for a trip time perturbed by two days. The maximum-net-mass problem is solved less accurately for trip times that are not multiples of 10 by relaxing the tolerances of the SQP termination criteria. Linear extrapolation of the past solutions is used to guide the design-space search for the optimal I_{sp} and power for the intermediate trip time problems. This procedure allows quick convergence to accurate solutions for trip times that are multiples of 10 days. The maximum-net-mass problem is solved accurately for trip times ranging from 80 to 200 days by 10-day increments by tightening the SQP termination criteria and eliminating the linear extrapolation scheme on I_{sp} and power. The same procedure is used to solve maximum-net-mass problems for trip times less than 72.5 days. Two such solutions have been obtained for trip times of 68 and 65 days, respectively. A summary of six representative maximum-net-mass solutions is presented in Table 2. The optimal P, I_{sp}, thrust and coast arc durations, and payload fraction for a given trip time are shown in this table.

The optimal payload fraction for the range of fixed-trip-time solutions is presented in Fig. 2. Each point on the curve represents an optimal combination of vehicle parameters and trajectory that maximizes the payload mass for a given total LEO-LLO trip time. As expected, the optimal payload fraction increases as the trip time increases. A sharp rise in payload is exhibited as the trip time is increased from 65 days to about 130 days. Increasing the trip time by 65 days from 65 to 130 days increases the payload fraction by 24.4%. Past 130 days, the performance curve begins to flatten. Increasing

Table 1 Maximum net mass solution vs minimum-propellant solution

Solution type	P, kW	I_{sp}, s	t_F, days	t_{escape}, days	Δt_{coast}, days	$t_{capture}$ days	m_F, MT	m_{net}, MT
Max m_{net}	3614.7	3641.4	72.50	58.16	3.26	11.08	98.96	71.37
Min m_{prop}	5000.0	5000.0	72.44	55.19	6.76	10.49	105.23	67.84

Table 2 Representative optimal vehicle-trajectory solutions

t_F, days	P, kW	I_{sp}, s	Δt_{QC_1}, days	Δt_e, days	Δt_{coast}, days	Δt_c, days	Δt_{QC_3}, days	m_{net}/m_0
65	3858.1	3435.6	38.27	13.66	3.21	6.30	3.56	0.555
90	3200.4	4032.3	52.56	18.85	5.74	7.88	4.96	0.625
120	2706.2	4664.2	70.55	25.68	6.27	10.72	6.78	0.678
150	2396.9	5245.3	88.56	32.63	6.58	13.61	8.62	0.713
180	2177.0	5772.3	106.53	39.62	6.85	16.54	10.46	0.738
200	2040.1	6023.6	117.78	43.77	7.06	19.74	11.65	0.750

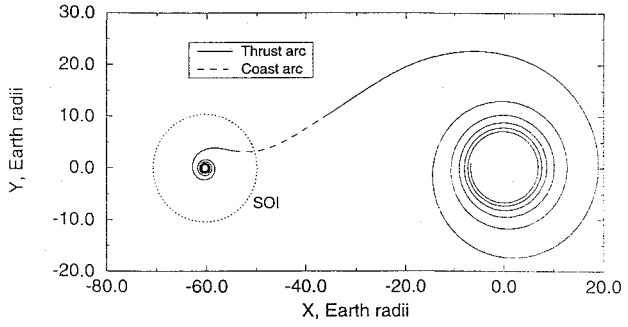

Fig. 1 Maximum-net-mass trajectory for t_F = 72.5 days—rotating coordinates.

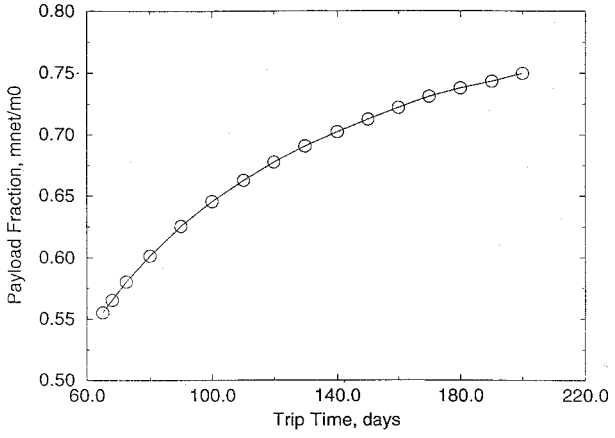

Fig. 2 Optimal payload fraction vs trip time.

the trip time by 70 days from 130 days to 200 days increases the payload fraction by only 8.5%. It appears that the payload fraction approaches a horizontal asymptote of about 0.77 as the trip time is increased past 200 days. However, this is only about a 2.7% increase in payload fraction from the 200-day solution and would probably not justify the increased trip time.

The corresponding optimal I_{sp} and power curves for the range of trip times are shown in Fig. 3. The optimal I_{sp} increases nearly linearly with trip time, and the optimal power decreases as the trip time increases. The 65-day solution approaches the lower limit for I_{sp} with an optimal I_{sp} of 3435.6 s and exhibits an optimal power level of 3858.1 kW. The optimal I_{sp} for the 200-day solution is 6023.6 s and is below the upper I_{sp} limit for xenon. The optimal power level for the 200-day solution is 2040.1 kW. The initial T/W and mass propellant flow rate are 1.33×10^{-4} and 410.0 kg/day, respectively, for the 65-day solution. As the trip time is increased and the optimal I_{sp} and power levels increase and decrease, respectively, the initial T/W ratio and mass flow rate decrease. For the 200-day solution, the initial T/W ratio in LEO is 4.41×10^{-5}, and the mass flow rate is reduced to 77.8 kg/day.

The numerically integrated segments of the optimal trajectories for the 65-day and 200-day solutions are shown in Figs. 4 and 5, respectively. The trajectories are displayed in an Earth-centered rotating coordinate system. The 65-day solution requires 38.2 days for the quasicircular transfer from LEO to GEO as approximated by Edelbaum's analytical expression. The numerically integrated trajectory, as shown in Fig. 4, requires 23.3 days to complete the GEO-HLO transfer. The escape spiral from GEO completes 5.3 revolutions about the Earth and lasts 13.6 days. The capture spiral completes 8.5 revolutions about the moon and terminates in the high circular lunar orbit. In comparison, the 200-day solution requires 117.8 days for the LEO-GEO quasicircular analytical transfer. The numerically integrated trajectory from GEO to HLO lasts 70.6 days, and the final HLO-LLO quasicircular transfer requires 11.6 days. During the numerically calculated escape spiral, the spacecraft completes 16.6 revolutions about the Earth before coasting for 7.2 days. The capture spiral to HLO completes 27.1 revolutions about the moon. The numerically integrated segment of the 200-day trajectory is displayed

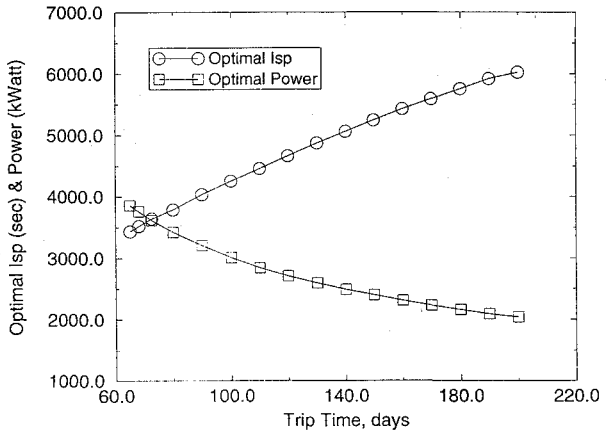

Fig. 3 Optimal I_{sp} and power vs trip time.

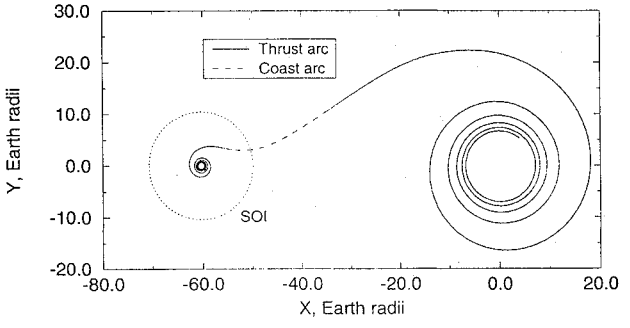

Fig. 4 Maximum-net-mass trajectory for t_F = 65 days—rotating coordinates.

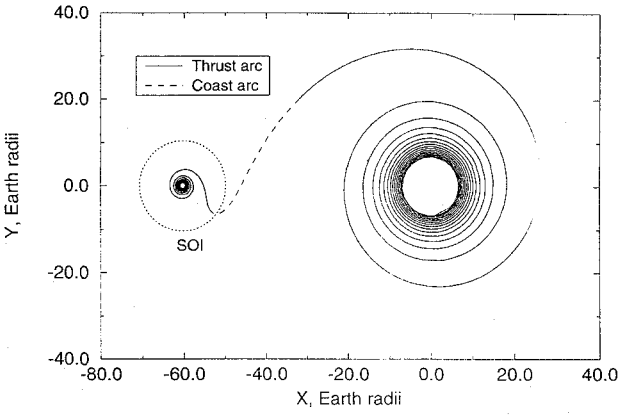

Fig. 5 Maximum-net-mass trajectory for t_F = 200 days—rotating coordinates.

in an Earth-centered inertial coordinate system in Fig. 6. During the 70.6-day transfer from GEO to HLO, the moon completes 2.6 revolutions about the Earth-moon center of mass. The initial position of the moon is indicated in the figure, and the subsequent 19.7-day moon-capture trajectory to HLO covers nearly three-fourths of a lunar orbit.

It should again be emphasized that these numerical results are for a range of NEP vehicles based on projected power and propulsion technology levels. The intent of this study is not to assess the impact of changing technology assumptions on the combined vehicle and trajectory optimization problem.

It can readily be shown[15] that the above maximum-net-mass problem is equivalent to the problem of minimizing the initial spacecraft mass in circular LEO for a fixed net mass to be delivered to circular LLO in a fixed transfer time. This alternative formulation was solved numerically by adding the unknown initial mass m_0 as a design variable and by adding another equality constraint to fix the desired net mass, m_{net}. The solution matched the optimal payload fraction to that of the equivalent maximum-net-mass problem to

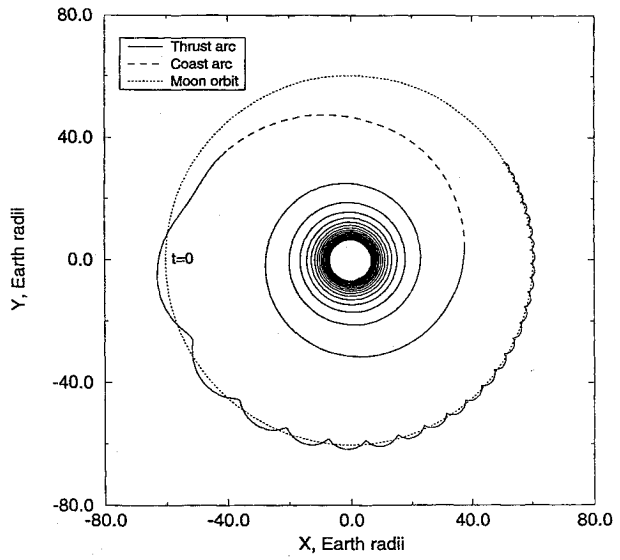

Fig. 6 Maximum-net-mass trajectory for t_F = 200 days—inertial coordinates.

seven significant figures, as expected. However, there appears to be no numerical advantage of solving the minimum-initial-mass problem.

Conclusions

A new combined vehicle and trajectory optimization problem has been formulated and solved for lunar missions using a low-thrust nuclear electric propulsion (NEP) spacecraft. The coupled vehicle sizing and trajectory optimization problem involves maximizing the payload for a fixed-trip-time, planar transfer from circular low Earth orbit to circular low lunar orbit. The NEP spacecraft sizing is accomplished by finding the optimal I_{sp}, input power P, and optimal thrust arc durations and steering histories for the Earth-escape and moon-capture spirals. The NEP vehicle model utilizes a projected technology level in power and propulsion system capabilities. Edelbaum's analytical expression for minimum-propellant, quasicircular transfers is utilized in order to reduce the computational load and improve the convergence properties of the problem.

Several optimal vehicle-trajectory combinations have been obtained for a range of trip times from 65 to 200 days spanning an order of magnitude in T/W ratio. As the trip time is increased, the optimal input power and I_{sp} steadily decrease and increase, respectively, which results in lighter, more efficient power and propulsion systems and therefore greater payload capabilities. The duration of the coast arc between the two powered spirals increases as the trip time is increased. The optimal payload fraction curve initially exhibits a sharp rise as the trip time is increased from 65 to 130 days. The performance levels off as the trip time is further increased from 130 to 200 days. The optimal payload fraction appears to approach a horizontal asymptote, and a further increase in trip time would probably not exhibit substantial payload increases.

Future research could involve studying the effect of uncertainty in the assumed technology level on the combined vehicle-and-trajectory optimization problem. The effects of altering the specific mass and tankage fraction could be investigated. A sensitivity analysis of important vehicle sizing parameters could also be performed.

The method presented allows a detailed analysis of the optimal interaction between vehicle system parameters and trajectory design variables. The vehicle-and-trajectory optimization approach used here has proven quite effective in solving a new and complex problem. The coupled optimization problem is important from the standpoint of both vehicle and mission design for a nuclear-electric-propulsion spacecraft.

Acknowledgments

This research was performed under the NASA Graduate Student Researchers Program and Grant NGT-50637. The authors would like to thank John Riehl at the NASA Lewis Research Center for his suggestions and contributions to this research project.

References

[1]Hack, K. J., George, J. A., and Dudzinski, L. A., "Nuclear Electric Propulsion Mission Performance for Fast Piloted Mars Missions," AIAA Paper 91-3488, Sept. 1991.

[2]Hack, K. J., George, J. A., Riehl, J. P., and Gilland, J. H., "Evolutionary Use of Nuclear Electric Propulsion," AIAA Paper 90-3821, Sept. 1990.

[3]Jaffe, L. D., "Nuclear-Electric Reusable Orbital Transfer Vehicle," *Journal of Spacecraft and Rockets*, Vol. 25, No. 5, 1988, pp. 375–381.

[4]Golan, O. M., and Breakwell, J. V., "Minimum Fuel Lunar Trajectories for Low-Thrust Power-Limited Spacecraft," AIAA Paper 90-2975, Aug. 1990.

[5]Enright, P. J., and Conway, B. A., "Discrete Approximations to Optimal Trajectories Using Direct Transcription and Nonlinear Programming," *Journal of Guidance, Control, and Dynamics*, Vol. 15, No. 4, 1992, pp. 994–1002.

[6]Gilland, J. H., "Mission and System Optimization of Nuclear Electric Propulsion Vehicles for Lunar and Mars Missions," NASA CR-189058, Dec. 1991.

[7]Jones, R. M., "Comparison of Potential Electric Propulsion Systems for Orbit Transfer," *Journal of Spacecraft and Rockets*, Vol. 21, No. 1, 1984, pp. 88–95.

[8]Burton, R. L., and Wassgren, C., "Time-Critical Low-Thrust Orbit Transfer Optimization," *Journal of Spacecraft and Rockets*, Vol. 29, No. 2, 1992, pp. 286–288.

[9]George, J. A., "Multimegawatt Nuclear Power Systems for Nuclear Electric Propulsion," AIAA Paper 91-3607, Sept. 1991.

[10]Stuhlinger, E., *Ion Propulsion for Spaceflight*, 1st ed., McGraw-Hill, New York, 1964, pp. 334–338.

[11]Szebehely, V. G., *Theory of Orbits, the Restricted Problem of Three Bodies*, 1st ed., Academic, New York, 1967, pp. 7–21.

[12]Bryson, A. E., and Ho, Y. C., *Applied Optimal Control*, Hemisphere, New York, 1975, pp. 47–89.

[13]Pierson, B. L., and Kluever, C. A., "A Three-Stage Approach to Optimal Low-Thrust Earth-Moon Trajectories," American Astronomical Society Paper 93-666, Vol. 18, No. 1, Aug. 1993.

[14]Edelbaum, T. N., "Propulsion Requirements for Controllable Satellites," *ARS Journal*, Vol. 31, No. 8, 1961, pp. 1079–1089.

[15]Kluever, C. A., "Optimal Low-Thrust Earth-Moon Trajectories," Ph.D. Dissertation, Iowa State Univ., Ames, IA, May 1993.

[16]Pierson, B. L., "Sequential Quadratic Programming and Its Use in Optimal Control Model Comparisons," *Optimal Control Theory and Economic Analysis 3*, North-Holland, Amsterdam, 1988, pp. 175–193.

[17]International Mathematics and Statistics Library, *User's Manual*, Version 1.1, Jan. 1989.

[18]Dixon, L. C. W., and Biggs, M. C., "The Advantages of Adjoint-Control Transformations When Determining Optimal Trajectories by Pontryagin's Maximum Principle," *Aeronautical Journal*, Vol. 3, March 1972, pp. 169–174.